Chapter 3

Caustics and wave chaos

3.1 The rainbow

Geometrical optics. The rainbow is created when sunlight is scattered by raindrops. A good model is the scattering of a parallel beam of light by a spherical drop. Using the laws of geometrical optics (reflection and refraction), the angular deviation θ of an incident light ray depends on its impact parameter b (see fig.3.1, left):

$$\theta(b) = 2i - 4r + \pi$$

where the angle of incidence is $i = \arcsin(b/R)$, and the refraction angle $r = \arcsin(b/nR)$. To get the angular distribution of the scattered light, we

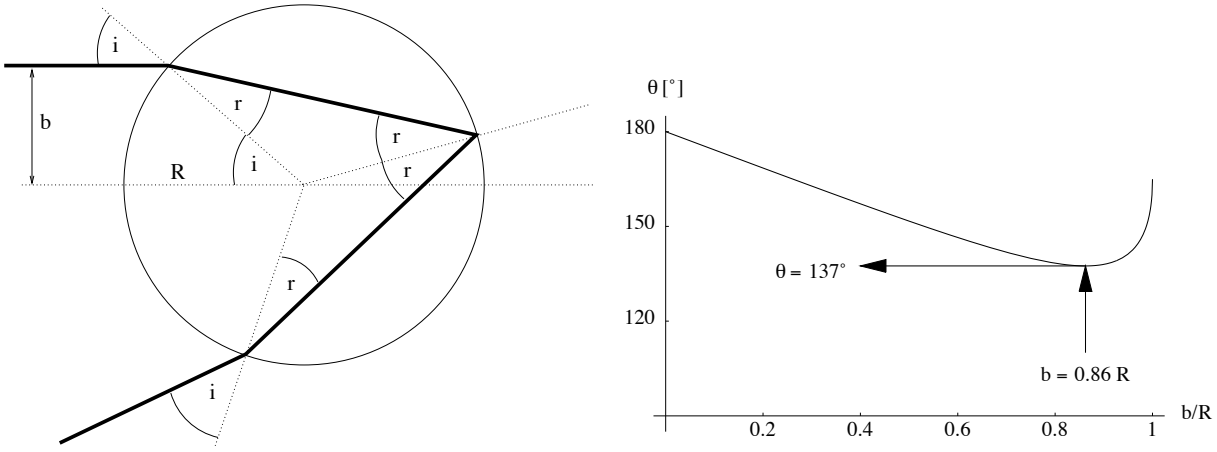

Figure 3.1: Deflection of light by a spherical water drop. Left: light ray; right: deflection angle vs. impact parameter.

backtrack the angle θ to the impact parameter b and assume that the incident

beam has a (uniform) distribution of impact sites across the drop cross section πR^2. The fraction of intensity $P(\theta)\mathrm{d}\theta$ scattered into the angle θ is therefore equal to $2\pi b\,\mathrm{d}b/\pi R^2$, the ratio between an annular area around the impact parameter b and the projected area of the drop. We thus get

$$P(\theta) = \frac{2b(\theta)}{R^2}\left|\frac{\mathrm{d}b}{\mathrm{d}\theta}\right| = \frac{2b(\theta)}{R^2}\frac{1}{|\mathrm{d}\theta/\mathrm{d}b|} \tag{3.1}$$

This distribution is shown in fig.3.2 and shows a diverging peak at the *rain-*

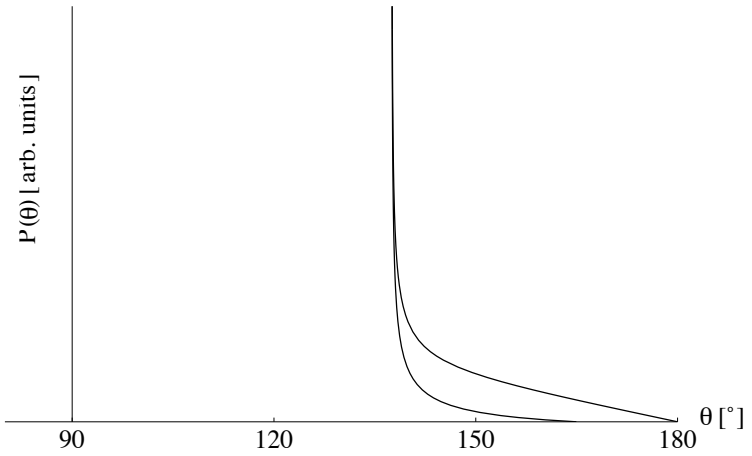

Figure 3.2: Angular distribution $P(\theta)$ (3.1).

bow angle θ_0 corresponding to the minimum value of $\theta(b)$. For this angle, the derivative $\mathrm{d}\theta/\mathrm{d}b$ vanishes which means that a large class of impact parameters contributes to scattering into this direction. For water drops, the refractive index is $n \approx 1.33$, and we get (DESCARTES, 17th century)

$$\theta_0 = 2\arccos\left[\frac{1}{n^2}\left(\frac{4-n^2}{3}\right)^{3/2}\right] \approx 137^\circ$$

For angles smaller than θ_0, no impact parameter may be found, and the angular distribution is zero. For angles larger than θ_0, two impact parameters contribute (this is the reason for the two curves in fig.3.2). Summing over both of them, the angular distribution in the vicinity of the maximum becomes

$$P(\theta) \approx \frac{2b_0}{R^2\sqrt{\alpha_0(\theta-\theta_0)}} \tag{3.2}$$

where $\alpha_0 = \frac{1}{2}\mathrm{d}^2\theta/\mathrm{d}b^2$ at the maximum.

The colors of the rainbow may be understood from the wavelength-dependence of the refractive index: this shifts the position θ_0 of the maximum intensity depending on the color. The second rainbow may be understood from a ray with two internal reflections inside the drop.

Wave picture. What becomes of the rainbow when we go beyond geometrical optics? In principle, the answer is straightforward: solve the scattering problem for electromagnetic waves from a dielectric sphere with index n. But the solution (MIE scattering) is quite cumbersome, and to get a plot for large droplets (radius R large compared to the wavelength), one has to sum a large number of terms.

We follow here a different, rather heuristic path. The angular distribution (3.1) looks much like a result obtained from the stationary phase approximation. We therefore look for functions $S(b;\,\theta)$ and $f(b)$ that yield (3.1) when the following integral is evaluated in the stationary phase approximation

$$I(\theta) = C \int \mathrm{d}b\, f(b)\, \exp[\mathrm{i}kS(b;\,\theta)] \tag{3.3}$$

The large parameter here is the wavenumber $k = 2\pi/\lambda$. The points of stationary phase are given by

$$\frac{\partial S}{\partial b} = 0$$

On the other hand, we have in the vicinity of the rainbow maximum

$$0 = \theta_0 - \theta + \alpha_0 (b - b_0)^2$$

This suggests the following form for the 'eikonal'

$$S(b;\,\theta) = (b - b_0)(\theta_0 - \theta) + \frac{\alpha_0}{3}(b - b_0)^3 + \text{const.}$$

The stationary phase method then yields the following value for the integral (3.3):

$$I(\theta) = C\sqrt{\frac{2\pi}{\mathrm{i}k}} \sum_i \left(\frac{\partial^2 S}{\partial b^2}\right)^{-1/2} f(b_i)\, \exp\left[\mathrm{i}kS(b_i;\theta)\right]$$

where the b_i are the stationary points. The second derivative is indeed of the form

$$\frac{\partial^2 S}{\partial b^2} = 2\alpha_0 (b - b_0) = \frac{\mathrm{d}\theta}{\mathrm{d}b}$$

If we choose the function $f(b) = \sqrt{b_0}/R$ and the constant $C = (k/2\pi)^{1/2}$, the square of $I(\theta)$ yields the angular distribution (3.2) given above (neglecting the interference terms).

But we can also express the integral $I(\theta)$ in terms of the AIRY function:

$$I(\theta) \;=\; \sqrt{\frac{kb_0}{2\pi R^2}}\int \mathrm{d}b\, \exp\left[\mathrm{i}k(b-b_0)(\theta_0-\theta)+\mathrm{i}k\frac{\alpha_0}{3}(b-b_0)^3\right]$$

Using the change of variables

$$t \;=\; (k\alpha_0)^{1/3}(b-b_0) \tag{3.4}$$

$$s \;=\; (k^2/\alpha_0)^{1/3}(\theta_0-\theta) \tag{3.5}$$

we find

$$I(\theta) = \frac{\sqrt{2\pi kb_0}}{R(k\alpha_0)^{1/3}}\mathrm{Ai}[s(\theta)] \tag{3.6}$$

The square of this function is plotted in fig.3.3 as a function of the parameter s. We see that the maximum of the scattered intensity is now finite. The 'dark

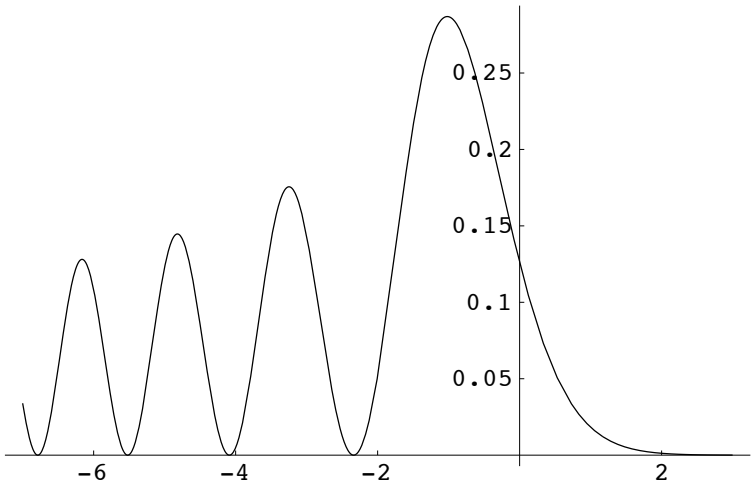

Figure 3.3: Squared AIRY function: intensity distribution across the rainbow.

side' of the rainbow, $s > 0$ or $\theta < \theta_0$ shows a small tail of intensity, while on the 'bright side', $\theta > \theta_0$, oscillations appear. These are due to the interference between two possible impact parameters that lead to the same scattering angle. The envelope of the oscillations is proportional to (see the asymptotic form (**??**) of the Airy function)

$$|I(\theta)|^2 \propto \frac{1}{\sqrt{\theta_0-\theta}}$$

this decay is the same as for the geometrical optics distribution (3.2).

The height of the 'rainbow peak' diverges like $k^{1/6}$ in the limit of geometrical optics. The angular width of the peak and of the oscillations is of the order of

$$\delta\theta \sim \left(\frac{\alpha}{k^2}\right)^{1/3} \sim (kR)^{-2/3}$$

and goes to zero in the geometrical optics limit.

3.2 The coffee cup caustic

As a second example, we switch to a caustic that occurs in "real space" (coordinates) as opposite to scattering directions (reciprocal space) of the rainbow.

3.2.1 Geometric rays

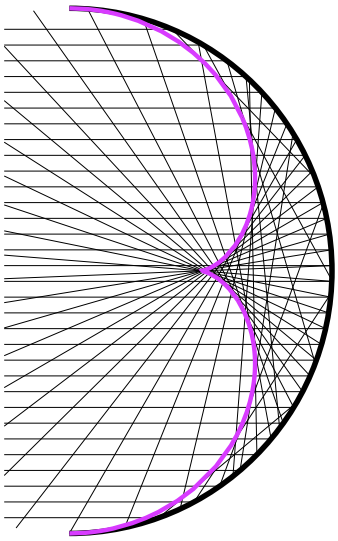

Fig.3.4. Family of rays in a coffee cup, forming a caustic.

The coffee cup caustic appears when parallel rays are reflected by a round (cylindrical) surface and hit a surface (the coffee surface or the bottom of the cup). One sees (Fig.3.4) two curves that meet in a bright tip. The curves are similar to the rainbow discussed above and are called "folds". The folds meet at the tip that is called a "cusp".
Parametrize incident ray by impact parameter $b = R\sin\theta$ or angular coordinate θ of impact point. The angle is measured with respect to the direction of the incident rays. The reflected ray makes an angle 2θ with respect to this direction. Follow the reflected ray and introduce the ray length s (measured from the cup surface towards the inside):

$$x = R\cos\theta - s\cos 2\theta \tag{3.7}$$

$$y = R\sin\theta - s\sin 2\theta \tag{3.8}$$

The coordinate x points along the incident direction, y is perpendicular to it. This is a mapping from the parameter space (s,θ) to the coordinate (or "control") space (x,y). If a family of rays (for different impact parameters) is traced, they form a curved envelope (magenta in Fig.3.4). This envelope is the *caustic*. It can be found from the condition that the mapping $(s,\theta) \mapsto (x,y)$ is singular. We calculate the Jacobian and its determinant:

$$J = \begin{pmatrix} \frac{\partial x}{\partial s} & \frac{\partial x}{\partial \theta} \\ \frac{\partial y}{\partial s} & \frac{\partial y}{\partial \theta} \end{pmatrix} = \begin{pmatrix} -\cos 2\theta & -R\sin\theta + 2s\sin 2\theta \\ -\sin 2\theta & R\cos\theta - 2s\cos 2\theta \end{pmatrix} \tag{3.9}$$

$$\det J = 2s - R\cos\theta \tag{3.10}$$

In parameter space, the coffeecup caustic is therefore given by an arc length $s = \frac{1}{2}R\cos\theta$, measured from the reflection point of the ray. In particular, we can already read off by taking $\theta = 0$ that the bright tip (cusp or focus) is located at $s = R/2$, half-way between the rim and the center of the cup.

The caustic in coordinate space is given by

$$x = R\cos\theta - \frac{R}{2}\cos\theta\cos 2\theta \tag{3.11}$$

$$y = R\sin\theta - \frac{R}{2}\cos\theta\sin 2\theta \tag{3.12}$$

In the following, we are interested in the behaviour near the cusp and expand for small θ. This gives

$$x = \frac{R}{2} + \frac{3}{4}R\theta^2, \qquad \theta \to 0 \tag{3.13}$$

$$y = \frac{7}{6}R\theta^3 \tag{3.14}$$

This illustrates that the cusp is given by the fractional parabola $y \sim \pm|x - x_c|^{3/2}$ with $x_c = R/2$.

3.2.2 Diffraction integral

For the wave optics of the coffee cup caustic, we suggest the following integral representation

$$\psi(x,y) = N\int_{-R}^{R} \mathrm{d}b\, \mathrm{e}^{\mathrm{i}kS(b\to x,y)} \tag{3.15}$$

where $S(b \to x, y)$ is the optical pathlength along a ray with impact parameter b, measured from a reference position in the incident family of parallel rays. By the construction of the arc length s of our geometric rays, we have

$$b = R\sin\theta, \qquad S(b\to x,y) = R\cos\theta + s, \tag{3.16}$$

taking as a reference the diameter $x = 0$ perpendicular to the incident rays. From Eq.(3.8), we can calculate s in terms of the final coordinates x, y and θ so that we finally get

$$\psi(x,y) = NR\int_{-\pi/2}^{\pi/2} \mathrm{d}\theta\, \cos\theta\, \exp \mathrm{i}k\left\{R\cos\theta + [(x - R\cos\theta)^2 + (y - R\sin\theta)^2]^{1/2}\right\} \tag{3.17}$$

Expand this for small θ, i.e., in the vicinity of the cusp, using the scaling (3.14) of the coordinates to separate the orders. The path length becomes, including terms up to order θ^4:

$$R\cos\theta + s \approx \frac{3R}{2} - x - \frac{R}{4}\theta^4 + 2x\theta^2 - 2y\theta \tag{3.18}$$

The first two terms do not come as a surprise: they describe the optical distance of the cusp from the reference plane and the rays that travel on average towards the left. We have shifted the origin of the x-axis to the cusp. The last three terms are all of order $\mathcal{O}(\theta^4)$.

In the integral (3.17), we can make the approximation $\cos\theta \approx 1$. (In the phase, there is the large factor kR that requires a higher precision.) With the substitution $(kR/4)^{1/4}\theta = t$, we get the following integral representation

$$\psi(x,y) \approx \frac{NR}{(kR/4)^{1/4}}\,\mathrm{e}^{\mathrm{i}k(3R/2-x)} \int_{-\infty}^{\infty} \mathrm{d}t\, \exp\mathrm{i}[-t^4 + \underbrace{(2kx)(kR/4)^{-1/2}}_{\bar{x}}\, t^2 - \underbrace{(2ky)(kR/4)^{-1/4}}_{\bar{y}}\, t] \tag{3.19}$$

The integral involved here can be expressed in terms of the Pearcey function Pearcey (1946); Nye (1999)

$$P(\bar{x},\bar{y}) = \int \frac{\mathrm{d}t}{\sqrt{2\pi}} \mathrm{e}^{\mathrm{i}(t^4+\bar{x}t^2+\bar{y}t)} \tag{3.20}$$

We note that the normalization factor N in Eq.(3.19) also depends on the wavelength, $N = (kR/2\pi\mathrm{i})^{1/2}$. We thus find with $\theta = \frac{3}{2}kR - \pi/4$

$$\psi(x,y) \sim (kR)^{1/4}\,\mathrm{e}^{-\mathrm{i}kx+\mathrm{i}\theta} P^*(-4\sqrt{kR}(x/R), 2\sqrt{2}(kR)^{1/4}y/R) \tag{3.21}$$

3.2.3 Pearcey diffraction pattern

The Pearcey function [Fig.3.5] gives a complex interference pattern with typical scales $\bar{x},\bar{y} \sim 1$ and an amplitude $\mathcal{O}(1)$. We thus read off from Eq.(3.21) that for short wavelengths, the cusp has a wave amplitude that diverges like $1/\lambda^{1/4}$, a sharper exponent than the scaling $1/\lambda^{1/6}$ that was found for the rainbow (diffraction at a "fold"). In the x-direction (along the average ray), the diffraction patches have a scale $\Delta x = \mathcal{O}(R\lambda)^{1/2}$, hence enhanced by the large factor $(R/\lambda)^{1/2}$ relative to the wavelength: the cusp is an example of "natural interference on the mesoscopic scale". In the y-direction (perpendicular to the main ray), the patches are thinner by a factor $(R/\lambda)^{-1/4}$.

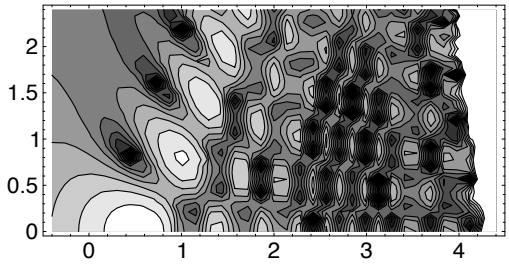

Figure 3.5: Modulus of the Pearcey function $P(x, y)$ [Eq.(3.20)]. The contours are drawn on logarithmic scale. The x-axis is horizontal, only the range $y > 0$ is shown (the function is symmetrically continued below the axis). The white fringe on the right is a numerical artefact, as are the "missing dark spots" in the region $3 < x < 4.5$. (The scaling of the coordinates may actually be wrong by a numerical factor.)

3.3 Approaches to Quantum Chaos

In this section, we shall present semiclassical methods that were developped since about 1970 in order to describe the quantum-mechanical energy spectrum of a classically chaotic system. We essentially follow Gutzwiller (1990) and Berry & Mount (1972).

The central tool is the so-called *trace formula*, first derived by GUTZWILLER in 1967. Thie formula relates the quantum-mechanical energy level density $n(E)$ to the spatial trace of the Green operator:

$$n(E) = -\frac{1}{\pi} \int \mathrm{d}q \, \mathrm{Im}\, G(q, q; E) \tag{3.22}$$

We get a tractable (though still complicated) expression when the semiclassical approximation for the Green function is used in this formula. In the following, we first prove (3.22) using elementary quantum mechanics and then approximate the Green function.

3.3.1 Green operator and function

For a quantum-mechanical system with HAMILTON operator $\hat{H}$, the GREEN operator is defined by

$$\left(E - \hat{H}\right) \hat{G} = \mathbb{1}$$

This equation is formally solved. Taking a complex energy $E + \mathrm{i}\,0$ with a positive (infinitesimal) imaginary part, we find

$$\mathrm{Im}\, \hat{G} = -\pi \mathbb{1}\, \delta\Big(E - \hat{H}\Big)$$

In the position representation, we have the expansion

$$G(q_B, q_A) = \langle q_B|\hat{G}|q_A\rangle = \sum_n \frac{\psi_n(q_B)\,\psi_n^*(q_A)}{E - E_n}$$

where the E_n are the energy eigenvalues and $\psi_n(q)$ the corresponding normalised wave functions. Putting here $q_B = q_A = q$ and integrating over q, we find

$$\int \mathrm{d}q\, G(q,q) = \sum_n \frac{1}{E - E_n}$$

For an energy $E + \mathrm{i}\,0$, the imaginary part gives

$$-\frac{1}{\pi}\mathrm{Im}\int \mathrm{d}q\, G(q,q) = \sum_n \delta(E - E_n) = n(E) \tag{3.23}$$

This is the energy level density: a series of δ peaks at the energy eigenvalues. For a continuous spectrum, the sum over n is actually an integral, and the level density becomes a continuous function.

3.3.2 The semiclassical propagator

We start with the semiclassical approximation to the time-dependent propagator.

The quantum-mechanical propagator $K(B, A) = K(q_B, t; q_A, 0)$ is equal to the probability amplitude that a particle reaches the position q_B at time t after starting from a position eigenstate localised in q_A at time 0.

The propagator thus solves the SCHRÖDINGER equation

$$\left(\mathrm{i}\hbar\partial_t + \frac{\hbar^2}{2m}\Delta_B - V(q_B)\right) K = 0$$

with the initial condition

$$\lim_{t\to 0} K(B, A) = \delta(q_B - q_A) \tag{3.24}$$

VAN VLECK **propagator**

As early as 1928, VAN VLECK wrote the following *Ansatz* for the propagator. It is inspired from the hydrodynamical formulation of the SCHRÖDINGER equation

$$K(B, A) = \frac{1}{(2\pi\mathrm{i}\hbar)^{D/2}} \sum_r \sqrt{C_r}\exp \mathrm{i}\,[R(B, A)/\hbar - \mu_r\pi/2] \tag{3.25}$$

To leading order in $\hbar \to 0$, we get from the SCHRÖDINGER equation the HAMILTON–JACOBI equation

$$\partial_t R + \frac{1}{2m} (\nabla_B R)^2 + V(q_B) = 0$$

Its solution is the action R (also called 'HAMILTON's principal function'). This can be calculated from classical dynamics.

In next-to-leading order, we find the continuity equation

$$\partial_t C_r + \frac{1}{m} \nabla_B \cdot (C_r \nabla_B R) = 0$$

where C_r plays the role of a (probability) density, and the momentum is $p_B = \nabla_B R(B, A)$ (standard relation from LAGRANGE mechanics). The amplitude C_r can hence also be calculated from classical dynamics.

It is easy to derive an explicit formula for the density in terms of the classical trajectories. Recall that the quantity

$$|K(B, A)|^2 \, \mathrm{d}q_B$$

gives the probability to reach a volume element $\mathrm{d}q_B$ around the final position q_B. Since probability is conserved along the classical trajectories, this probability is equal to the probability to start with the correct initial momentum p_A (see figure 3.6). This is given by

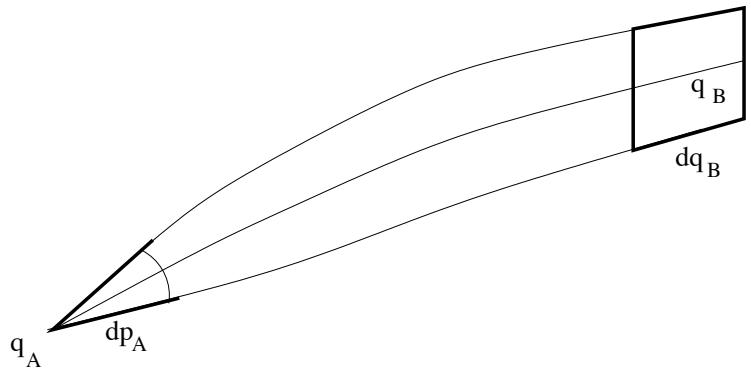

Figure 3.6: Final position q_B and initial momentum p_A.

$$g(p_A)\mathrm{d}p_A = \frac{\mathrm{d}p_A}{(2\pi\hbar)^D}$$

with the momentum distribution $g(p_A)$. For an initially localised particle, we know from quantum mechanics that its momentum distribution is flat. We thus find

$$|K(B, A)|^2 = \frac{1}{(2\pi\hbar)^D} \frac{\partial(p_A)}{\partial(q_B)}$$

The last fraction is to be read as a JACOBI determinant. Using the relation $p_A = -\nabla_A R(B,A)$, we also get

$$|K(B,A)|^2 = \frac{1}{(2\pi\hbar)^D} \det\left(-\frac{\partial^2 R(B,A)}{\partial q_A \, \partial q_B}\right)$$

Comparing to (3.25) and neglecting the interference between different classical paths, it follows

$$C_r = \det\left(-\frac{\partial^2 R(B,A)}{\partial q_A \, \partial q_B}\right)$$

Note that the sum over different classical paths leading to the same final position q_B already appears in the classical theory.

We still have to check the initial condition at $t \to 0$. At short times, the MASLOV index (that counts the caustics touched by the classical trjaectory) is zero. We get the action from the Lagrangian

$$\begin{aligned}
&\lim_{t\to 0} \int_0^t \mathrm{d}t' \left(\frac{m}{2}\dot{q}^2 - V(q)\right) \\
&= \frac{mt}{2}\dot{q}^2 - V(q_A)t = \frac{mt}{2}\left(\frac{q_B - q_A}{t}\right)^2 - V(q_A)t \\
&= \frac{m\,(q_B - q_A)^2}{2t}
\end{aligned}$$

In the last line, we have only kept the leading term in the short-time limit. Note that the potential energy disappears in this limit: the particle behaves as if it were free. The matrix relating initial momentum and final position is thus given by

$$\frac{\partial^2 R(B,A)}{\partial q_A \, \partial q_B} = -\frac{m}{t}\mathbb{1}$$

and we eventually find

$$t \to 0: \quad K(B,A) = \left(\frac{m}{2\pi \mathrm{i}\hbar\, t}\right)^{D/2} \exp\left[\frac{\mathrm{i}m}{2\hbar\, t}(q_B - q_A)^2\right]$$

This is a complex gaussian representation of the δ-function: only for $q_B = q_A$, the phase does not oscillate rapidly. We check the normalisation using the FRESNEL integral

$$\int \mathrm{d}t\, \mathrm{e}^{\mathrm{i}t^2/2} = \sqrt{2\pi\mathrm{i}}$$

and find indeed

$$\int \mathrm{d}q\, K(B,A) = \left(\frac{m}{2\pi\mathrm{i}\hbar\, t}\right)^{D/2} \left(\frac{2\pi\mathrm{i}\hbar\, t}{m}\right)^{D/2} = 1$$

All quantities appearing in the VAN VLECK propagator (3.25) are now specified.

MASLOV **index**

Along a classical path, the matrix $C_{ij} = -\partial^2 R/\partial q_{Ai}\,\partial q_{Bj}$ may become singular. Recall that if we displace the final position by δq_B, the initial momentum has to change by δp_A with

$$\delta p_{Ai} = \frac{\partial p_{Ai}}{\partial q_{A_j}}\,\delta q_{Bj} = C_{ij}\,\delta q_{Bj}$$

If the path touches a caustic (envelope of the paths), a momentum displacement p_A does not change the final point q_B in first order. In other words, the volume transported along the path goes to zero. This means that at least one eigenvalue of inverse matrix $(C_{ij})^{-1}$ vanishes. This happens at isolated points along the path (called '*conjugate points*' by Gutzwiller (1990)). After the caustic, the matrix C is no longer singular, and its determinant C of C_{ij} has changed sign. This has to be taken into account when the square root is taken in (3.25). We adopt the convention that $C = |\det(C_{ij})|$ and that a phase $-\pi/2$ is added for each conjugate point on the trajectory. This corresponds to the phase chosen in (3.25), where the MASLOV index $\mu_r =$ counts the number of conjugate points (caustics) along the trajectory. We note that μ_r is piecewise constant between conjugate points and does not contribute to derivatives. Since it only changes the phase of the propagator, it does not either enter the probability density. The previous calculations for the action $R(B, A)$ and the density $C_r(B, A)$ thus remain valid.

3.3.3 Semiclassical GREEN function

We now change from the time-dependent propagator to the energy-dependent GREEN function. Gutzwiller (1990) gives the definition

$$G(B, A; E) = \frac{1}{\mathrm{i}\hbar}\int_0^\infty \mathrm{d}t\, K(B, A)\,\mathrm{e}^{\mathrm{i}Et/\hbar} \tag{3.26}$$

which looks like a FOURIER transform of the propagator.

It is simple to establish the connection to the standard definition of the GREEN function for the stationary SCHRÖDINGER equation. Up to a factor $\hbar^2/2m$, this function satisfies

$$\left(E + \frac{\hbar^2}{2m}\Delta_B - V(q_B)\right) G = \delta(q_B - q_A) \tag{3.27}$$

We may write the equations for the propagator $K(B, a)$ also in the following form: the propagator is the causal solution of

$$\left(\mathrm{i}\hbar\partial_t + \frac{\hbar^2}{2m}\Delta_B - V(q_B)\right) K = \mathrm{i}\hbar\delta(t)\,\delta(q_B - q_A)$$

'Causal' means here that $K(B,A) = 0$ for $t < 0$. Integrating over a small time interval around $t = 0$ gives back the initial condition (3.24). We may now take the standard time FOURIER transform and divide by $\mathrm{i}\hbar$. The result is identical to eqs. (3.26, 3.27).

Putting the VAN VLECK propagator (3.25) into (3.26), we find

$$G(B,A;E) = \frac{2\pi}{(2\pi\mathrm{i}\hbar)^{D/2+1}} \times \\ \times \sum_r \int_0^\infty \mathrm{d}t \, \sqrt{C_r} \exp \mathrm{i} \left[R(B,A)/\hbar - \mu_r \pi/2 + Et/\hbar \right]$$

In the semiclassical limit, it is reasonable to solve this integral with the stationary phase method. Stationarity gives

$$\frac{\partial R(B,A)}{\partial t} + E = 0 \tag{3.28}$$

Eq.(3.28) defines a time t_r such that the classical trajectory that reaches the point q_B has the energy E. We may compare this relation to the HAMILTON–JACOBI theory. For a time-independent HAMILTON function, one separates the time-dependence of the action $R(B,A)$ by writing

$$R(B,A) = S(B,A) - Et$$

where E is energy along the path. We recover (3.28) when the time-derivative is taken.

The second derivative at the stationary point is

$$\left. \frac{\partial^2 R}{\partial t^2} \right|_{t_r} = - \left. \frac{\partial E}{\partial t} \right|_{t_r} = - \left(\frac{\partial t_r}{\partial E} \right)^{-1}$$

Conversely, we have $\partial S / \partial E = t_r$ and hence

$$\left. \frac{\partial^2 R}{\partial t^2} \right|_{t_r} = - \left(\frac{\partial^2 S}{\partial E^2} \right)^{-1}$$

Finally, the stationary phase result for the GREEN function is

$$G(B,A;E) = \frac{2\pi}{(2\pi\mathrm{i}\hbar)^{\frac{D+1}{2}}} \times \\ \times \sum_r \left[-\frac{\partial^2 S_r}{\partial E^2} C_r \right]^{1/2} \exp \mathrm{i} \left[S(B,A)/\hbar - \mu_r \pi/2 \right] \tag{3.29}$$

Example: free space

In free space, the reduced action at fixed energy E is given by (note that the momentum is fixed to $p = \sqrt{2mE}$):

$$S(B,A) = \int_A^B p(q;E)\,\mathrm{d}q = \sqrt{2mE}\;|q_B - q_A|$$

We get the same result from the time-dependent action using the value $t_r = m\,|q_B - q_A|\,/p$ for the stationary time:

$$\begin{aligned} S(B,A) &= R(q_B,t_r;q_A,0) + Et_r \\ &= \frac{m(q_B-q_A)^2}{2t_r} + \frac{p^2}{2m}\frac{m\,|q_B-q_A|}{p} = p\,|q_B-q_A| \end{aligned}$$

The MASLOV index is zero $\mu_r = 0$ for a point source in free space. As noted above, the density is identical to the short-time limit

$$C_r = \left(\frac{m}{t_r}\right)^D = \frac{p^D}{|q_B-q_A|^D}.$$

The second derivative becomes

$$\frac{\partial^2 S}{\partial E^2} = -\frac{1}{4}\sqrt{\frac{2m}{E^3}}\,|q_B-q_A| = -\frac{m^2}{p^3}\,|q_B-q_A|\,,$$

and we get the final result

$$G(B,A;E) = \frac{2\pi m}{(2\pi \mathrm{i}\hbar)^{\frac{D+1}{2}}}\left(\frac{p^{D-3}}{|q_B-q_A|^{D-1}}\right)^{1/2} \mathrm{e}^{\mathrm{i}p|q_B-q_A|/\hbar}$$

In three dimensions with $r = |q_B - q_A|$, $k = p/\hbar$,

$$D = 3: \quad G(B,A;E) = -\frac{2m}{\hbar^2}\frac{\mathrm{e}^{\mathrm{i}kr}}{4\pi r}, \tag{3.30}$$

which is the correct GREEN function for the HELMHOLTZ equation. The factor $2m/\hbar^2$ is due to the factor in front of the LAPLACE operator in (3.27).

In one dimension,

$$D = 1: \quad G(B,A;E) = -\frac{2m}{\hbar^2}\frac{\mathrm{i}}{2k}\mathrm{e}^{\mathrm{i}kr} \tag{3.31}$$

in agreement with the results of problem **??**.

For other dimensions D, one needs a uniform approximation to the GREEN function[1].

Finally, we compute the level density in free space and $D = 3$. The GREEN function only depends on the position difference $q_B - q_A$, hence $G(q, q; E)$ is independent of q, and the integration over q gives the volume V of the system. The energy level density per volume is now

$$\frac{n(E)}{V} = -\frac{1}{\pi}\mathrm{Im}\, G(q, q; E) = \frac{mk}{2\pi^2\hbar^2}$$

This result is typically obtained by counting plane wave states in a cube of side length L using periodic boundary conditions (momentum spacing $\mathrm{d}k_i = 2\pi/L$, $i = 1, 2, 3$):

$$\frac{n(E)}{L^3} = L^{-3}\left(\frac{L}{2\pi}\right)^3 \frac{k^2\,\mathrm{d}k\,\mathrm{d}\Omega}{\mathrm{d}E}$$

Summing over all directions replaces the solid angle $\mathrm{d}\Omega \mapsto 4\pi$. Furthermore, $k\,\mathrm{d}k = \mathrm{d}(k^2/2) = (m/\hbar^2)\,\mathrm{d}E$, and we find indeed

$$\frac{n(E)}{L^3} = \left(\frac{1}{2\pi}\right)^3 \frac{4\pi mk}{\hbar^2} = \frac{mk}{2\pi^2\hbar^2}$$

A more interesting case is a particle confined by a potential. We start first in one dimension and show that we get back the quantisation rule of BOHR and SOMMERFELD.

3.3.4 Quantisation and classical periodic orbits

In the semiclassical GREEN function $G(q, q; E)$, we need closed classical paths $q \mapsto q$ starting and ending in q. These come in two types: paths of 'zero length' and 'finite loops'.

[1] See Berry & Mount (1972):

$$\begin{aligned} G(B, A; E) &= \frac{1}{\mathrm{i}\hbar(2\pi\hbar)^{\frac{D-1}{2}}} \sum_r \left| -\frac{\pi S_r(B, A)}{2\hbar} \frac{\partial^2 S_r(B, A)}{\partial E^2} C_r(B, A) \right|^{1/2} \times \\ &\quad \times H^{(1)}_{D/2-1}(S_r(B, A)/\hbar - \mu_r\pi/2) \end{aligned}$$

with the HANKEL function $H^{(1)}_\nu$. Because of

$$\begin{aligned} H^{(1)}_{1/2}(x) &= -\mathrm{i}\,\mathrm{e}^{\mathrm{i}x}(2/\pi x)^{1/2} \\ H^{(1)}_{-1/2}(x) &= \mathrm{e}^{\mathrm{i}x}(2/\pi x)^{1/2} \end{aligned}$$

the uniform approximation reduces to the expressions (3.30, 3.31) in three and one dimensions.

Contribution of zero length paths

We denote their contribution to the level density by $n_0(E)$. The MASLOV index is zero. Hence

$$\begin{aligned} n_0(E) &= -\frac{1}{\pi}\mathrm{Im}\,\frac{2\pi}{(2\pi\mathrm{i}\hbar)^{\frac{D+1}{2}}}\times \\ &\quad \times\int \mathrm{d}q\,\lim_{q_B\to q}\left(-\frac{\partial^2 S}{\partial E^2}C\right)^{1/2}\exp \mathrm{i}S(q_B,q;E)/\hbar \end{aligned}$$

Note that the classical path exists only if $E > V(q)$ (classically allowed region RI). Furthermore, the momentum has the local value $p(q) = \sqrt{2m(E-V(q))}$. Otherwise, the motion looks like that of a free particle.

Using the 1D GREEN function (3.31) for free space, we get

$$\begin{aligned} n_0(E) &= \frac{2m}{\pi\hbar^2}\mathrm{Im}\int_{RI}\mathrm{d}q\frac{\mathrm{i}\hbar}{2p(q)}\lim_{\delta q\to 0}\exp\left[\mathrm{i}p(q)\delta q/\hbar\right] \\ &= \frac{m}{\pi\hbar}\int_{RI}\frac{\mathrm{d}q}{p(q)} = \frac{T(E)}{2\pi\hbar} \end{aligned} \tag{3.32}$$

where $T(E)$ is the classical time for the bound motion at energy E (*e.g.*, the energy E_1 in figure 3.7).

If the energy is such that the motion is not bound (like E_2 in figure 3.7), the time $T(E)$ is infinite. We can however define the change of level density with respect to a free particle. From (3.31) and the trace formula, we have $n_{\mathrm{free}}(E) = mL/\pi\hbar p$ where L is the volume (length) of the system. We can thus write

$$\begin{aligned} \Delta n(E) &= n_0(E) - n_{\mathrm{free}}(E) \\ &= \frac{m}{\pi\hbar}\int \mathrm{d}q\left(\frac{1}{\sqrt{2m(E-V(q))}} - \frac{1}{\sqrt{2mE}}\right) \end{aligned}$$

The advantage of this formula is that its integrand goes to zero in the asymptotic region $q\to\infty$ where the potential is zero. For energies above bound states, this is the only correction to the level density since there are no finite closed loops.

For comparison, we calculate the contribution of zero-length loops in $D = 3$. Using the GREEN function (3.30), we have

$$\begin{aligned} n_0(E) &= \frac{2m}{4\pi^2\hbar^2}\lim_{\delta q\to 0}\mathrm{Im}\int_{RI}\mathrm{d}^3q\frac{\exp \mathrm{i}p(q)\delta q/\hbar}{\delta q} \\ &= \frac{4\pi m}{(2\pi\hbar)^3}\int_{RI}\mathrm{d}^3q\,p(q) \end{aligned}$$

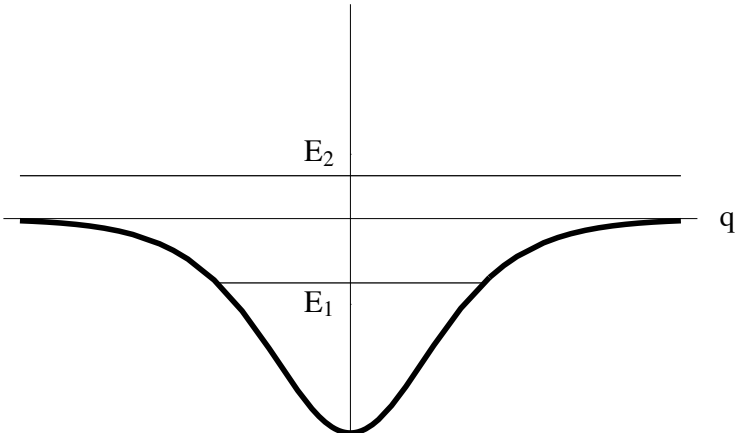

Figure 3.7: One-dimensional potential well. No closed loops for E_2, closed loops for E_1.

This result may be compared to the standard 'recipe' of statistical mechanics 'Each quantum state occupies a phase space volume equal to $h^D = (2\pi\hbar)^D$'. This rule gives

$$\begin{aligned} n(E) &= \frac{1}{(2\pi\hbar)^3}\int \mathrm{d}^3q \int \mathrm{d}^3p\, \delta(H(p,q)-E) \\ &= \frac{1}{(2\pi\hbar)^3}\int \mathrm{d}^3q \int \mathrm{d}^3p\, \frac{\partial p}{\partial E}\delta(p-p(q;E)) \\ &= \frac{4\pi m}{(2\pi\hbar)^3}\int_{RI} \mathrm{d}^3q\, p(q;E) \end{aligned}$$

using $\partial p/\partial E = m/p$ and spherical coordinates for the momentum integral. We thus get the zero-length level density $n_0(E)$.

Nontrivial closed loops

Let us call their contribution $n_p(E)$. Evaluating the integral over q in the trace formula in the stationary phase approximation, we find a stationary point at

$$0 = \frac{\partial S(q,q;E)}{\partial q} = \left.\frac{\partial S}{\partial q_B}\right|_q + \left.\frac{\partial S}{\partial q_A}\right|_q = p_B - p_A$$

This gives a particular closed loop starting and ending at q with the same momentum, *i.e.*, a *periodic trajectory* or periodic orbit. GUTZWILLER's trace formula thus links the energy level density to a sum over the periodic orbits of the classical system.

'It has long been known that the periodic orbits are of fundamental importance in semiclassical mechanics (Einstein 1917, Brillouin 1926, Keller 1958), but their precise meaning is only now becoming clear as a result of this work of Gutzwiller (1971).'

(Berry & Mount, 1972, p.388)

The action for a single circuit around a closed orbit (in the positive sense) is

$$S_1(E) = 2\int_{q_1}^{q_2} \mathrm{d}q'\, p(q'), \qquad q_{1,2}: \text{ turning points}$$

We note that it is independent of the particular point q on the orbit.

For the density C_r along the orbit, we need second derivatives of the action. To start with, we distinguish between starting and end point and get for the path $q_A \to q_2 \to q_1 \to q_B$ (nearly one return)

$$S(q_B, q_A; E) = \int_{q_A}^{q_2} \mathrm{d}q'\, p(q') + S_1(E) + \int_{q_1}^{q_B} \mathrm{d}q\, p(q')$$

The differentiation gives

$$\frac{\partial^2 S}{\partial q_B\, \partial q_A} = -\frac{\partial p(q_A)}{\partial q_B} + \frac{\partial p(q_B)}{\partial q_A} = 0 + 0 = 0$$

because the positions $q_{A,B}$ are independent variables. We must have forgotten something...

This second derivative appeared in the time-dependent propagator, when we related changes of final positions and initial momenta: $\partial p_A/\partial q_B = -\partial^2 R(B,A)/\partial q_B\, \partial q_A$. There, the time t was kept constant, while here, we deal with the energy-dependent action $S(q_B, q_A; E)$. Gutzwiller (1990) remarks that one has to vary both position *and energy*:

$$\left.\frac{\partial p_A}{\partial q_B}\right|_t = \left.\frac{\partial p_A}{\partial q_B}\right|_E + \left.\frac{\partial p_A}{\partial E}\right|_{q_B} \frac{\partial E}{\partial q_B}, \tag{3.33}$$

while the derivative $\partial E/\partial q_B$ is fixed by the constraint that the time $t = \partial S/\partial E = \text{const.}$. The differentiation of this relation gives

$$0 = \frac{\partial t}{\partial q_B} = \frac{\partial^2 S}{\partial E\, \partial q_B} + \frac{\partial^2 S}{\partial E^2}\frac{\partial E}{\partial q_B}.$$

Putting that into (3.33), we find the 'transformation matrix on the energy surface' (Gutzwiller, 1990)

$$C_{ij} = \left.\frac{\partial p_A}{\partial q_B}\right|_t = -\frac{\partial^2 S}{\partial q_A\, \partial q_B} + \frac{\partial^2 S}{\partial q_A\, \partial E}\frac{\partial^2 S}{\partial q_B\, \partial E}\left(\frac{\partial^2 S}{\partial E^2}\right)^{-1} \tag{3.34}$$

The (squared) amplitude of the GREEN function (3.29) thus becomes

$$-\frac{\partial^2 S}{\partial E^2}\det(C_{ij}) =$$
$$-\left(\frac{\partial^2 S}{\partial E^2}\right)^{1-D}\det\left(-\frac{\partial^2 S}{\partial q_A\,\partial q_B}\frac{\partial^2 S}{\partial E^2}+\frac{\partial^2 S}{\partial q_A\,\partial E}\frac{\partial^2 S}{\partial q_B\,\partial E}\right)$$

In $D=1$, the determinant is trivial. We already found that the first term in parentheses vanishes. The second term is found from

$$\frac{\partial^2 S}{\partial q_B\,\partial E}=\frac{\partial p_B}{\partial E}=\frac{\partial}{\partial E}\sqrt{2m(E-V(q_B))}=\frac{m}{p_B}$$

and a similar result involving $-m/p_A$. This result is independent of the number of periods needed to reach q_B.

One dimension: BOHR–SOMMERFELD quantisation

We can now let $q_B \to q_A$ and find the level density $n_r(E)$ for an orbit with $r\in\mathbb{Z}\backslash\{0\}$ returns

$$n_r(E)=\frac{m}{\pi\hbar}\mathrm{Re}\int_{q_1}^{q_2}\frac{\mathrm{d}q}{|p(q)|}\exp\mathrm{i}\left[rS_1(E)/\hbar-r\pi\right]$$

Two phase jumps of $-\pi/2$ at the turning points are included for each period. We observe that the result (3.32) for the zero length loops may be recovered by putting $r=0$. Furthermore, the one-loop action $S_1(E)$ is independent of q, and the integration gives one half classical period. The full semiclassical level density is therefore

$$\begin{aligned} n(E) &= n_0(E)+n_p(E) \\ &= \frac{T(E)}{2\pi\hbar}\sum_{r\in\mathbb{Z}}\exp\mathrm{i}r\left[S_1(E)/\hbar-\pi\right] \end{aligned}$$

This sum may be evaluated with the help of the POISSON summation formula

$$\sum_{r\in\mathbb{Z}}\mathrm{e}^{\mathrm{i}rw}=2\pi\sum_{n\in\mathbb{Z}}\delta(w-2\pi n)$$

We thus find

$$\begin{aligned} n(E) &= \frac{T(E)}{\hbar}\sum_{n\in\mathbb{Z}}\delta\left[S_1(E)/\hbar-\pi-2\pi n\right] \\ &= T(E)\sum_{n\geq 0}\delta\left[S_1(E)-(2n+1)\pi\hbar\right] \\ &= \sum_{n\geq 0}\delta\left(E-E_n\right) \end{aligned}$$

This is a series of δ-peaks with the energy eigenvalues E_n given by the BOHR–SOMMERFELD quantisation rule:[2]

$$S_1(E_n) = (n + \tfrac{1}{2})2\pi\hbar$$

In the semiclassical regime, the spacing between the energy levels is equal to the inverse classical period:

$$2\pi\hbar = \delta E \frac{\partial S_1}{\partial E} \quad \Longrightarrow \quad \delta E = \frac{2\pi\hbar}{T(E)}$$

A large period therefore corresponds to an increased density of the energy levels. For the hydrogen atom, *e.g.*, the period approaches infinity for $E \nearrow 0$; and the spectrum shows indeed an accumulation of levels there.

Finally, if the discrete levels are too close together to be resolved, one gets an 'averaged' level density with a value (one state per level spacing)

$$\overline{n}(E) = \frac{1}{\delta E} = \frac{T(E)}{2\pi\hbar} = n_0(E)$$

This is precisely the contribution of zero-length orbits.

3.3.5 The spectrum of classically chaotic systems with isolated periodic orbits

In integrable or separable systems, periodic orbits occur in families and cover some part of the coordinate space. This leads to a discrete spectrum.

The more generic case is a non-integrable system. Periodic orbits are then isolated in space. They contribute distinctive features to the energy spectrum that are superimposed on a smooth background (the contribution of the zero length paths).

Classical stability analysis

We introduce a local coordinate system $q = (q_0, q_1, q_2)$ with $q_{1,2} = 0$ along on the periodic orbit. If we take a point $\bar{q}$ on the periodic orbit, then the action $S_1(q, q; E)$ for a single circuit along the periodic orbit is independent of $\bar{q}_0$, similar to the one-dimensional case. A trajectory starting with initial position q_A and momentum p_A slightly offset from a point $\bar{q}, \bar{p}$ on the periodic orbit will hopefully stay in the vicinity of the orbit and end up at a final position (q_B, p_B)

[2]The transformation of the δ-function makes use of the relation $\partial S_1/\partial E = T(E)$.

slightly offset from $\bar{q}, \bar{p}$. The action of this path is given by $S(q_B, q_A; E)$. To first order in the displacements $\delta q_{A,B} = q_{A,B} - \bar{q}$, we have

$$\begin{aligned} \delta p_{Ai} &= -\frac{\partial^2 S}{\partial q_{Ai}\,\partial q_{Aj}}\delta q_{Aj} - \frac{\partial^2 S}{\partial q_{Ai}\,\partial q_{Bj}}\delta q_{Bj} \\ \delta p_{Bi} &= \frac{\partial^2 S}{\partial q_{Bi}\,\partial q_{Aj}}\delta q_{Aj} + \frac{\partial^2 S}{\partial q_{Bi}\,\partial q_{Bj}}\delta q_{Bj} \end{aligned}$$

with indices $i, j = 1, 2$. All derivatives are evaluated along the periodic orbit. Gutzwiller (1990) writes this linear system in the abbreviated form

$$\begin{aligned} \delta p_A &= -a\,\delta q_A - b\,\delta q_B \\ \delta p_B &= b^T\,\delta q_A + c\,\delta q_B \end{aligned}$$

with real 2×2 matrices a, b, c containing the second derivatives of the action (b^T is the transpose of b).

A more geometric interpretation of what happens in the vicinity of the periodic orbit is provided by the relation between initial and final deviations. This is also a linear system with the matrices

$$\begin{aligned} \delta q_B &= A\,\delta q_A + B\,\delta p_A \\ \delta p_B &= C\,\delta q_A + D\,\delta p_A \end{aligned}$$

It is an easy calculation that these matrices are given by

$$\begin{aligned} A &= -b^{-1}a & B &= -b^{-1} \\ C &= b^T - cb^{-1}a & D &= -cb^{-1} \end{aligned}$$

provided the matrix b (with the mixed second derivatives) is nonsingular.

Let us consider the eigenvalues λ of this linear transformation that may loosely be associated with the LYAPUNOV exponents of the dynamics in phase space. (A more precise definition will be introduced below.) The characteristic polynomial of the linear transformation is ($\mathbb{1}$ is the 2×2 identity matrix)

$$\begin{aligned} F(\lambda) &= \det\begin{pmatrix} A - \lambda\mathbb{1} & B \\ C & D - \lambda\mathbb{1} \end{pmatrix} \\ &= \det\begin{pmatrix} -b^{-1}a - \lambda\mathbb{1} & -b^{-1} \\ b^T - cb^{-1}a & -cb^{-1} - \lambda\mathbb{1} \end{pmatrix} \end{aligned} \tag{3.35}$$

To simplify this determinant, we subtract from the second row the first one, multiplied with c. Furthermore, factoring out b^{-1} from the first row and expanding the determinant along the first row, we find

$$F(\lambda) = \det\begin{pmatrix} -b^{-1}a - \lambda\mathbb{1} & -b^{-1} \\ b^T + \lambda c & -\lambda\mathbb{1} \end{pmatrix} \tag{3.36}$$

$$= \frac{1}{\det(b)} \det\Big(\lambda a + \lambda^2 b + b^T + \lambda c\Big) \tag{3.37}$$

From this expression, we can read off that $F(0) = 1$, *i.e.*, the linear transformation between $\delta q_A, \delta p_A$ and $\delta q_B, \delta p_B$ preserves the volume of phase space (LIOUVILLE's theorem). Furthermore, since the characteristic polynomial $F(\lambda)$ is real (the matrices a, b, c being real), the eigenvalues are either real or complex conjugate pairs. Finally, one can also check that whenever λ is a solution of $F(\lambda) = 0$, then this is also true for $1/\lambda$.

The following cases are now distinguished by Gutzwiller (1990):

elliptic orbit: the eigenvalues are pure phase factors $\lambda = \mathrm{e}^{\mathrm{i}\chi}, \mathrm{e}^{-\mathrm{i}\chi}$;

(direct) hyperbolic orbit: [3] the eigenvalues are real $\lambda = \mathrm{e}^{\chi}, \mathrm{e}^{-\chi}$;

loxodromic orbit: the eigenvalues are $\lambda = \mathrm{e}^{\pm u \pm \mathrm{i}v}$ with real u, v.

For each degree of freedom transverse to the orbit, one gets a pair of eigenvalues. We see that loxodromic orbits occur only with three degrees of freedom at least.

The geometric meaning of these cases is the following:

elliptic orbit: the phase space volume is rotated after one circuit along the orbit, but its aspect ratio is preserved. The angle χ describes the rotation angle per roundtrip. An elliptic periodic orbit is also called 'stable' because in the long time limit, neighbouring points remain at a finite distance from the orbit.

hyperbolic orbit: one direction in phase space gets stretched by a factor e^{χ}, while the other one is shrunk by the opposite factor $\mathrm{e}^{-\chi}$. In this context, the quantity χ may be identified with the LYAPUNOV exponent for the stretched direction. A hyperbolic orbit is also called 'unstable' because the distance from the orbit increases without limits in the direction corresponding to the positive LYAPUNOV exponent χ.

[3] **Inverse hyperbolic orbits** have eigenvalues $\lambda = -\mathrm{e}^{\chi}, -\mathrm{e}^{-\chi}$.

An elliptic orbit with $\chi = 0, \pi$ is called a *parabolic* orbit: in this case, a small cube in phase space is mapped onto itself (or its reflected image) without rotation nor distortion. This case is typical for an integrable system according to GUTZWILLER, but it is non-generic.

Contribution to the level density

After these preparations for the classical dynamics, we can face the contribution of a periodic orbit to the quantum-mechanical level density:

$$n(E) = -\mathrm{Im}\, \frac{2}{(2\pi \mathrm{i}\hbar)^{\frac{D+1}{2}}} \times \tag{3.38}$$
$$\times \int \mathrm{d}q \sum_r \left[-\frac{\partial^2 S_r}{\partial E^2} C_r \right]^{1/2} \exp \mathrm{i} \left[S_r(q,q;E)/\hbar - \mu_r \pi/2 \right]$$

We have to integrate over the points q on closed orbits. In the hope that the positions $\bar{q}$ along the periodic orbit will give a dominant contribution, the action $S_r(q,q;E)$ will be expanded in the vicinity of this particular orbit. For points $\bar{q}$ on the orbit, the action gives a value $S_r(E) = S_r(\bar{q},\bar{q};E)$ independent of $\bar{q}$.

The variation to first order in $\delta q = q - \bar{q}$ is zero because the orbit is closed: initial $p_A = -\partial S_r/\partial q_A$ and final momenta $p_B = \partial S_r/\partial q_B$ are equal. We now use the local coordinate system centred on the orbit introduced above and consider a point displaced by $\delta q = q - \bar{q}$ transverse to the orbit (only the $1, 2$ components are nonzero). To second order, this gives a variation of the action

$$\delta S_r \;=\; \frac{1}{2} \left(\frac{\partial^2 S}{\partial q_{Ai}\, \partial q_{Aj}} + 2 \frac{\partial^2 S}{\partial q_{Ai}\, \partial q_{Bj}} + \frac{\partial^2 S}{\partial q_{Bi}\, \partial q_{Bj}} \right) \delta q_i\, \delta q_j$$

where all derivatives are calculated at the point $\bar{q}$ on the periodic orbit.

We consider first a single roundtrip around the orbit. Then we can use the matrices a, b, c introduced before and express the second variation of the action as

$$\delta S_1 = \frac{1}{2} \delta q \cdot \left(a + b + b^T + c \right) \cdot \delta q \tag{3.39}$$

Here, we wrote the matrices in a symmetrised form since this is appropriate for the quadratic form δS_1. The integration with respect to q (or, equivalently, δq) is now a multi-$(D-1)$-dimensional FRESNEL integral, since the phase $S_1/\hbar$ is a quadratic form of the displacements δq. We neglect the variation of the amplitude factor transverse to the orbit and get

$$\int \mathrm{d}^2 q\, \mathrm{e}^{\mathrm{i}\delta S_1/\hbar} = \frac{(2\pi \mathrm{i}\hbar)^{\frac{D-1}{2}}}{\det \left(a + b + b^T + c \right)^{1/2}} \tag{3.40}$$

If the (symmetric) matrix $a+b+b^T+c$ has a number μ of negative eigenvalues, then the square root is resolved by taking the absolute value and adding a phase factor $\mathrm{e}^{-\mathrm{i}\mu\pi/2}$. We observe that the determinant in (3.40) also appears in the characteristic polynomial $F(\lambda)$ defined in (3.35). More precisely, we have

$$\det\Big(a+b+b^T+c\Big) = F(1)\det(b) = F(1)\det\left(\frac{\partial^2 S}{\partial q_{Ai}\,\partial q_{Bj}}\right).$$

Finally, we have to work out the amplitude factor in the GREEN function in the trace formula (3.41). From (3.34), we know that the density C_r is a determinant containing second derivatives of the action with respect to position (like the matrices a, b, c and mixed derivates. These may be calculated by differentiating the time-independent HAMILTON–JACOBI equation:

$$H\left(\frac{\partial S}{\partial q_B}, q_B\right) = E$$

In the local coordinate system along the periodic orbit, the differentiation with respect to the (initial) coordinate q_A gives (with indices $\alpha, \beta = 0, 1, 2$)

$$\frac{\partial H}{\partial p_{B\alpha}}\frac{\partial^2 S}{\partial q_{B\alpha}\,\partial q_{A\beta}} = 0$$

This already shows that the full matrix with the mixed derivatives of the action is singular, because the velocity vector $v_{B\alpha} = \partial H/\partial p_{B\alpha}$ is mapped onto zero. Furthermore, in the local coordinates, we know that the velocity points in the 0-direction: $v_{B\alpha} = (|v_B|, 0, 0)$. We thus conclude that the elements with $\alpha = 0$ of the matrix $\partial^2 S/\partial q_{B\alpha}\,\partial q_{A\beta}$ vanish.

Finally, knowing the momentum $p_{B\alpha} = \partial S/\partial q_{B\alpha}$, we find by taking the derivative with respect to the energy E

$$\frac{\partial^2 S}{\partial q_{B\alpha}\,\partial E} = \frac{m}{|p_B|}\delta_{\alpha,0}$$

The second matrix appearing in (3.34) therefore has only a single nonzero element at the $0,0$ position.

We can now expand the determinant C_r (3.34) with respect to the first row and find

$$\begin{aligned}
&-\frac{\partial^2 S}{\partial E^2}\det(C_{\alpha\beta}) \\
&= -\left(\frac{\partial^2 S}{\partial E^2}\right)^{1-D}\det\begin{pmatrix} -m^2/|p_A|\,|p_B| & 0 & 0 \\ C_{10} & & -\dfrac{\partial^2 S}{\partial E^2}\dfrac{\partial^2 S}{\partial q_{Ai}\,\partial q_{Bj}} \\ C_{20} & & \end{pmatrix} \\
&= (-1)^{D-1}\frac{m^2}{|p_A|\,|p_B|}\det\left(\frac{\partial^2 S}{\partial q_{Ai}\,\partial q_{Bj}}\right)
\end{aligned}$$

where the C_{j0} are irrelevant matrix elements. We note again that this result is independent of the number of round trips. For a single passage along the periodic orbit, we recover the determinant of the matrix b:

$$-\frac{\partial^2 S}{\partial E^2}\det(C_{\alpha\beta}) = (-1)^{D-1}\frac{m^2}{|p_A|\,|p_B|}\det(b)$$

Putting everything together, we find the following expression for the contribution of a single passage (in the positive sense) of the periodic orbit:

$$n_1(E) = -\mathrm{Im}\,\frac{\mathrm{e}^{\mathrm{i}[S_1(E)/\hbar-\mu_1\pi/2]}}{\pi\mathrm{i}\hbar}\int \mathrm{d}\bar{q}_0 \frac{m}{|p(\bar{q}_0)|}\frac{1}{\sqrt{(-1)^{D-1}F(1)}} \tag{3.41}$$

Gutzwiller (1990) mentions in passing that $F(1)$ is independent of $\bar{q}_0$ and takes it outside the integral. We are then left with the integration of $\mathrm{d}\bar{q}_0/\bar{v}$ that gives the period $T(E)$ for a single roundtrip along the orbit (the 'primitive period').

The function $F(1)$ may be calculated from the knowledge of the eigenvalues of the phase-space mapping along the orbit. For each degree of freedom transverse to the orbit, we get a pair of eigenvalues λ. The discussion is most simple with $D = 2$. Then a single eigenvalue pair $\lambda, 1/\lambda$ is sufficient to characterise the stability of the orbit. The characteristic polynomial $F(1)$ is calculated from

$$\begin{aligned} F(1) &= (1-\lambda)\left(1-\lambda^{-1}\right) \\ &= 2-\left(\lambda+\lambda^{-1}\right) \end{aligned}$$

For the elliptic and hyperbolic orbits introduced above, we thus find[4]

$$\begin{aligned} \text{elliptic:} \quad & F(1) = 2\,(1-\cos\chi) = 4\sin^2(\chi/2) \\ \text{(direct) hyperbolic:} \quad & F(1) = 2\,(1-\cosh\chi) = -4\sinh^2(\chi/2) \end{aligned}$$

For an elliptic orbit, we thus have

$$n_1(E) = \mathrm{Im}\,\frac{T(E)}{2\pi\hbar}\frac{\mathrm{e}^{\mathrm{i}w}}{\sin(\chi/2)}$$

with $w = S_1(E)/\hbar - \mu_1\pi/2$. A similar result holds for the hyperbolic orbit. Note that this expression does not hold for an integrable system (parabolic orbit with $\chi = 0$).

[4]For an inverse hyperbolic orbit: $F(1) = 4\cosh^2(\chi/2)$.

Stable orbit: sharp energy levels

What is the contribution of multiple roundtrips of the orbit? The action and the MASLOV index get multiplied by r, the number of roundtrips. The phase-space mapping is the r'th iteration of a single circuit mapping, and therefore its eigenvalues are λ^r. The quantity χ (in the exponent of λ) therefore gets replaced by $r\chi$. The sum over multiple roundtrips along an elliptic orbit therefore is

$$n_{\text{e.o.}}(E) = \text{Im}\,\frac{T(E)}{2\pi\hbar}\sum_{r=1}^{\infty}\frac{\text{e}^{\text{i}rw}}{\sin(r\chi/2)}$$

To compute the sum, we make the expansion

$$\frac{1}{\sin(r\chi/2)} = 2\text{i}\text{e}^{-\text{i}r\chi/2}\sum_{l=0}^{\infty}\text{e}^{-\text{i}lr\chi}$$

This expansion is made to converge when we add a negative imaginary part to the stability angle χ. For each term of the sum over l we now get a geometric series. Its summation gives

$$n_{\text{e.o.}}(E) = \text{Im}\,\frac{\text{i}T(E)}{\pi\hbar}\sum_{l=0}^{\infty}\frac{1}{\text{e}^{-\text{i}[w-(2l+1)\chi/2]}-1}$$

This expression has a pole whenever $w-(2l+1)\chi/2$ is a multiple of 2π. Knowing that χ has a negative imaginary part, we find the following expansion around the poles

$$\begin{aligned}\frac{1}{\text{e}^{-\text{i}[w-(2l+1)\chi/2]}-1} &= \sum_{n\in\mathbb{Z}}\frac{1}{-\text{i}[w-(2l+1)\chi/2-2\pi n]}\\ &= \sum_{n\in\mathbb{Z}}\Big(\pi\delta[w-(2l+1)\chi/2-2\pi n]+\\ &\qquad +\text{i}\mathcal{P}\frac{1}{w-(2l+1)\chi/2-2\pi n}\Big)\end{aligned}$$

The level density is now determined by the δ-function, and we get

$$\begin{aligned}n_{\text{e.o.}}(E) &= \sum_{n,l\geq 0}\delta(E-E_{n,l})\\ \text{with}\qquad & S_1(E_{n,l}) = \left[(n+\tfrac{\mu_1}{4})2\pi+(l+\tfrac{1}{2})\chi\right]\hbar\end{aligned}\qquad (3.42)$$

The (stable) elliptic orbit hence leads to a series of sharp, discrete energy eigenvalues that are characterised by two quantum numbers n and l. The quantum number n is analogous to what we saw in one dimension. The 'stability angle' χ may be seen as a correction to phase jump $\mu_1\pi/2$ associated with the

MASLOV index. Finally, to interpret the quantum number l, we may speculate that the neighbourhood of the stable periodic orbit is 'bound' to it as in a harmonic potential well (this is clear if we linearise the equations of motion around the orbit, for example). The harmonic well contributes a transverse energy $(l+\frac{1}{2})\hbar\omega$ to the eigenvalues. From the quantisation rule (3.42), we read off that $\omega = \chi/T(E_{n,l})$.

Unstable orbit: resonances

Finally, what changes when the orbit is hyperbolic, *i.e.*, unstable? The contribution of an r-fold roundtrip is found by a similar reasoning to be

$$n_r(E) = -\mathrm{Im}\,\frac{T(E)}{2\pi\mathrm{i}\hbar}\frac{\mathrm{e}^{\mathrm{i}rw}}{\sinh(r\chi/2)}$$

To sum this over the number of roundtrips r, we observe that the distinct features in the level density arise from the behaviour for large r in the sum. In this regime, we may replace the $\sinh(\chi/2)$ by its asymptotic form $\frac{1}{2}\mathrm{e}^{\chi/2}$. The sum then becomes again a geometric series, but in distinction to the stable orbit, we get denominators with a resonant behaviour (without poles for real w):

$$\frac{1}{\mathrm{e}^{-\mathrm{i}w+\chi/2}-1} = \mathrm{i}\sum_{n\in\mathbb{Z}}\frac{w-2\pi n-\mathrm{i}\chi/2}{(w-2\pi n)^2+\chi^2/4}$$

This expansion in the vicinity of the poles is valid when the dimensionless action w is much larger than the LYAPUNOV exponent χ and when χ is small compared to unity.

The energy spectrum thus shows a series of Lorentzian resonances:

$$n_{\mathrm{h.o.}}(E) = \frac{T(E)}{2\pi}\sum_{n\geq 0}\frac{\hbar\chi}{(S_1(E)-(n+\frac{\mu_1}{4})2\pi\hbar)^2+\hbar^2\chi^2/4} \tag{3.43}$$

The resonances are centered at the energies E_n from the BOHR–SOMMERFELD quantisation rule:

$$S_1(E_n) = (n+\tfrac{\mu_1}{4})2\pi\hbar$$

Their width $\hbar\Gamma_n$ is related to the LYAPUNOV exponent by

$$\hbar\Gamma_n \approx \frac{\hbar\chi}{T(E_n)}$$

The periodic unstable orbit thus leads to a series of resonances in the energy range where the orbit exists. Their spacing is given by $\hbar/T(E)$. The resonances may be individually resolved if the LYAPUNOV exponent (that determines their width) is much smaller than unity, *i.e.*, if the orbit is not too unstable.

Bibliography

M. V. Berry & K. E. Mount (1972). Semiclassical approximations in wave mechanics, *Rep. Prog. Phys.* **35**, 315–397.

M. C. Gutzwiller (1971). Periodic orbits and classical quantization conditions, *J. Math. Phys.* **12** (3), 343–58.

M. C. Gutzwiller (1990). Chaos in Classical and Quantum Mechanics. volume 1 of *Interdisciplinary Applied Mathematics*. Springer, New York.

J. F. Nye (1999). *Natural focusing and fine structure of light*. Institute of Physics Publishing, Bristol.

T. Pearcey (1946). The structure of an electromagnetic field in the neighbourhood of a cusp of a caustic, *Phil. Mag.* **37** (268), 311–17.